Oxygen partial pressure effects on the magnetron sputtered WO_3 films

G Merhan Muğlu [1], E Gür[1]

[1]Department of Physics, Faculty of Science, Atatürk University, 25240, Erzurum, Turkey.

E-mail: *emregur@atauni.edu.tr*

Abstract. Electrochromism is changing color of a substance in response to the applied an external electric field and the phenomenon is reversible. WO_3 is very attractive material due to its electrochromic properties as well as it is also attractive for many different applications such as gas sensors, phosphorous screen, textile, glass industry. In this study, it is aimed to provide optimization of the optical and structural characteristics of WO_3 by changing the growth parameters mainly the oxygen partial pressure. The partial pressure of oxygen was changed with increments of 0.7 mTorr. For the analysis, X-ray Diffraction (XRD), absorption, Raman spectroscopy measurements were used. When O_2 gas increased, peaks belong to the WO_3 was observed in XRD patterns at the 2 theta angles of 23.0, 11.0, 23.5 and 28.5 angles corresponding to the (002), (020) and (220) planes, respectively. This shows that there is a significant effect of increasing O_2 partial pressure in the formation of WO_3 films. The bandgap energy of the WO_3 thin films are found to be around 3.0 eV. Raman measurements showed vibrational modes of W-O-W stretching and bending modes which shows small shifts depending on the partial pressures of the O_2. Obtained results indicated that better crystal structure is obtained with higher O_2 gas partial pressure.

1. Introduction

Tungsten trioxide thin films have been extensively studied because of their potential application in electrochromic devices. The optical properties of these films can be changed in a reversible and persistent way under the influence of an applied voltage [1]. Electrochromism refers to the reversible change of color of thin films due to a small change in the voltage. This is important for smart windows and display applications [2-4]. It is widely accepted that the electrochromic process involves the simultaneous injection (or extraction) of electrons and charge compensating ions into interstitial sites of the WO_3 matrix [5]. For the polycrystalline films, the injected electrons behave as free-carriers leading to an increase in the near infrared reflectivity [6]. Nevertheless, scattering of the excess free electrons by extended defects, leads to lower reflectivity in this region [7].

Various methods have been used to prepare WO_3 thin films, including thermal evaporation [8,10,13,14], chemical vapor deposition (CVD) [12,15], sputtering [9,11,16,17,18,19] and pulsed laser deposition (PLD) [20,21]. In this study WO_3 thin film were deposited on the glass substrate by R.F magnetron sputtering a 99.9% pure tungsten target.

Content from this work may be used under the terms of the Creative Commons Attribution 3.0 licence. Any further distribution of this work must maintain attribution to the author(s) and the title of the work, journal citation and DOI.
Published under licence by IOP Publishing Ltd

2. Experimental

RF magnetron sputtering has advantageous of having high deposition rates, sputtering of insulating targets, low power and low pressure operation conditions. WO_3 thin films were deposited on the Si (111), Si(100), ITO substrates by R.F. magnetron sputtering using a 99.9% pure 2'' diameter W target reactively. The vacuum chamber was evacuated to 5×10^{-7} Torr base pressure before the deposition. Both argon and oxygen flows were controlled by mass flow controllers. The total pressure in the deposition chamber was kept constant at 12-15 mTorr. It was aimed to provide optimization of the optical and structural characteristics of WO_3 by changing the growth parameters mainly the oxygen partial pressure. The partial pressure of oxygen was changed with increments of 0.7 mTorr. While the applied power to the target was kept constant at 100 W and the substrate temperature was maintained at 350K.

Initially the deposition parameters were optimized to obtained WO_3 films with high transparency. Later, all the parameters except the deposition time were kept constant. The deposition parameters are listed in Table 1.

Table 1. R.F. sputtered parameters used for deposition of WO_3 thin films.

Growth material	**Base Pressure (torr)**	**Growth Pressure (mTorr)**	**Temperature (Celcius)**	**Gas1 Ar (sccm)**	**Gas2 O_2 (sccm)**	**Growth Rate (A^o/s)**	**Growth Time**	**Substrate**
WO_3	$1{,}5 \times 10^{-6}$	15,70	330	12.5	**0.5**	1,5	130	Si (111) Si (100) İTO glass
WO_3	6×10^{-7}	18,35	311	12.5	**1.5**	0,2	-	Si (111) Si (100) İTO glass
WO_3	$1{,}3 \times 10^{-6}$	18,88	300	12.5	**1**	0,6	54	Si (111) Si (100) İTO glass
WO_3	$7{,}8 \times 10^{-7}$	20,3	300	12.5	**2**	0,1	60	Si (111) Si (100) İTO glass

3. Results and Discussion

Increasing O_2 partial pressure led to the formation of XRD peaks for WO_3 films grown on ITO and the p-Si substrate. No XRD peak was observed for the thin films grown at the lowest oxygen partial pressure. XRD Peaks belong to the WO_3 films was observed at 23.0, 11.0, 23.5 and 28.5 angles corresponding to the (002), (020) and (220) planes, respectively. The peak intensity ratio of the of (002) plane to the other planes in films grown on the ITO substrate significantly has increased with increasing O_2 partial pressure. This shows that there is a significant effect of increasing O_2 partial pressure in the formation of WO_3 films. XRD results suggests that better crystal structure is possible by increasing O_2 partial pressure in WO_3 thin films.

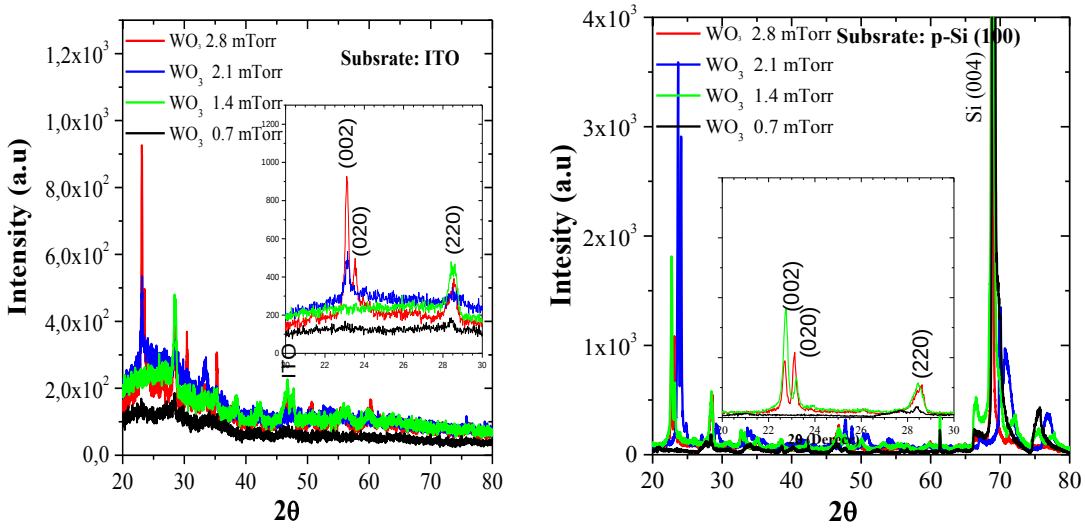


Figure 1. XRD pattern of WO_3 thin films grown as depending on to O_2 partial pressure.

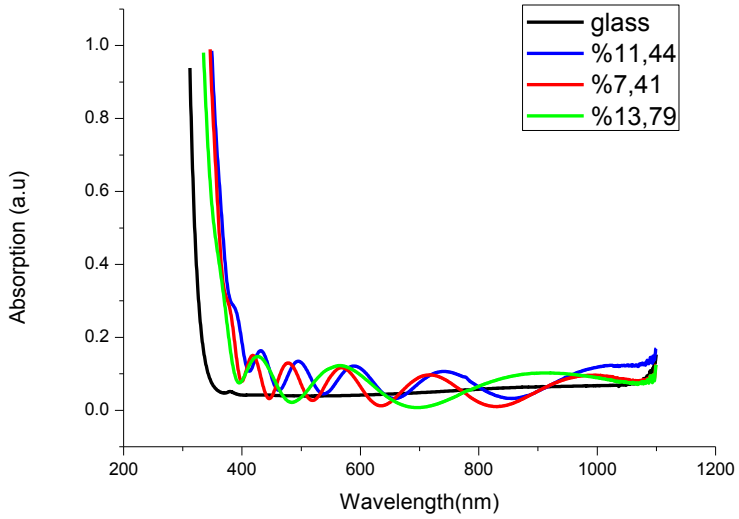


Figure 2. Absorption pattern of WO_3 thin films grown depending on to O_2 partial pressure.

Absorption plot of films that is grown at the highest O_2 partial pressure from the grown WO_3 thin films is shown in Fig.2. Starting around 400 nm, absorption spectra increases corresponding to the near band edge absorption of the grown WO_3 thin films. In the figure above, absorption spectrum of the pure glass substrates has shown in the plot which is used as the reference [20]. Very sharp absorption band edges of the sputtered WO_3 thin films suggest the successful high quality of the grown thin films.

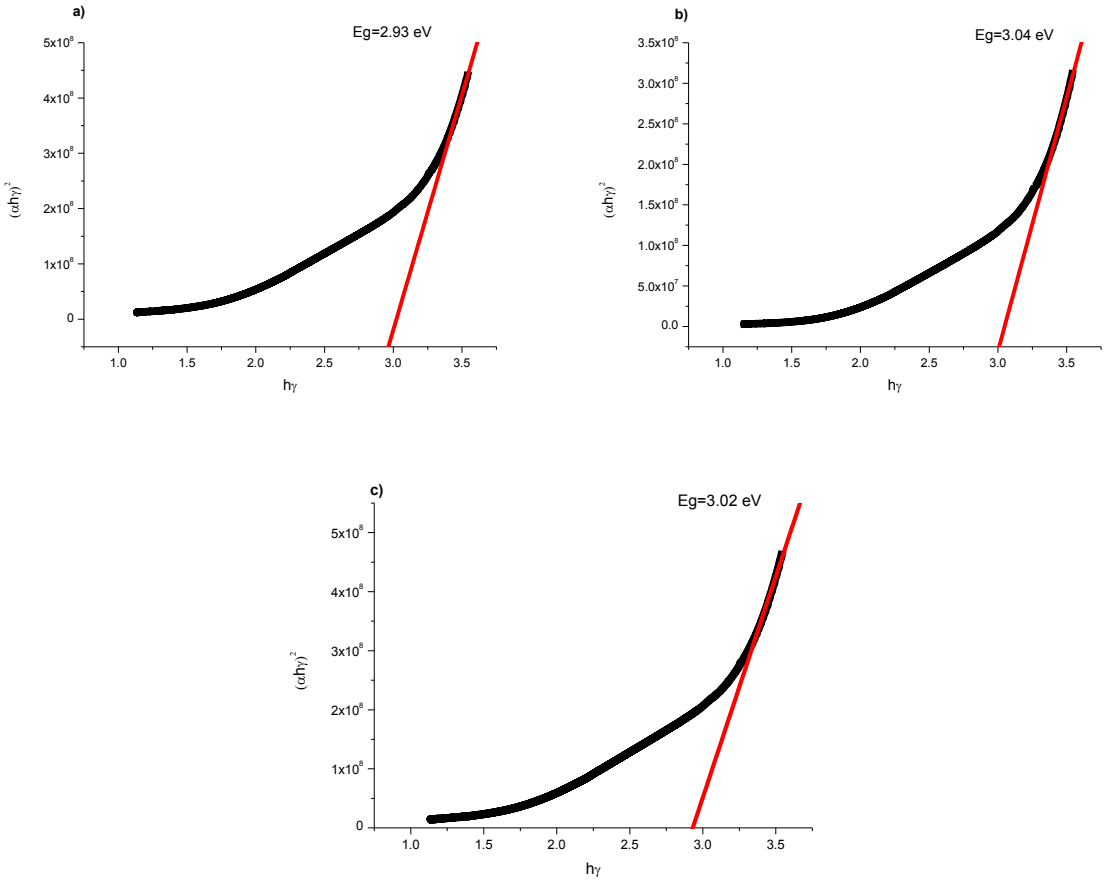


Figure 3.The absorbance spectra were used to determine optical band gap energies of WO_3 on glass substrate.

Bandgap of the WO_3 thin films is shown in Fig.3 by using the following relation for near band edge optical absorption of semiconductors,

$$\alpha = (\frac{K}{h\gamma})(h\gamma - E_g)^z \quad (1)$$

where $\boldsymbol{\alpha}$ is absorption co-efficient, hν is the photon energy, K is a constant, E_g is the optical band gap and n is a constant (n equals 1/2 for allowed direct transitions) [25-29]. Fig. 3 shows the plot of $(\alpha h\nu)^2$ versus hν for 4.45% O_2 partial pressure, 11.44% O_2 partial pressure, 13.79% O2 partial pressure on glass substrate thin films; the linear portion of the curve is extrapolated to the energy (hν) axis and the intercept gives the value of optical band gap E_g of the film [30]. The optical band gap values for 4.45% O_2 on glass substrate, 11.44% O_2, 13.79 % O_2 thin films, determined from Fig. 3(a)-(c) as the 2.93 eV, 3.04 eV, 3.02 eV respectively.

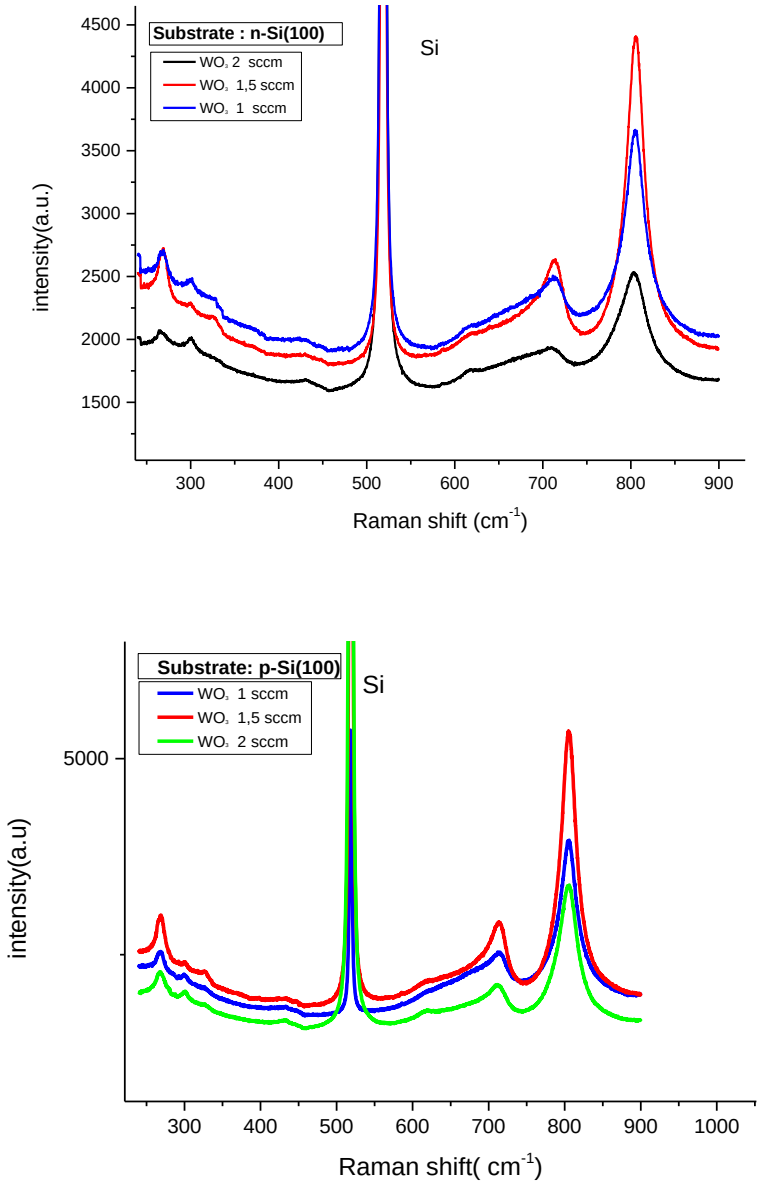


Figure 4. Raman spectra of WO_3 thin films grown depending on to O_2 partial pressure.

The Raman spectroscopy is effective in revealing structural features and structural transitions in WO_3 owing to its high sensitivity to the small changes in the lattice positions of the tungsten atoms. The WO_3 exhibits the following sequence of crystal phases with increasing temperature: triclinic , monoclinic , orthorombic , tetragonal [21]; in particular, bulk WO_3 is monoclinic-γ between 20°C and 330°C and it is orthorombic-β between 330°C and 740°C [22]. When Raman spectrum of the as prepared WO_3 thin films are examined, it is seen four well defined peaks located at 807, 710, 327, and 267 cm^{-1}. The high-frequency peaks at 807 and 710 cm^{-1} were attributed to the W–O–W stretching vibration mode, while the low frequency ones (i.e., 327 and 267 cm^{-1}) were attributed to the W–O–W bending mode. The peaks shown in the present study similar to those for monoclinic WO_3 thin films [23,24]. WO_3 thin films were

not shown for 0.7 mTorr. The details of the Raman peaks, wavenumbers and Full Width at Half Maximum (FWHM) obtained is given in table 1 and 2, respectively.

Table 2. Peak analysis of WO_3 thin films in Raman Spectroscopy

Si n-tipi	**% 4.45 O_2 (0.5 sccm)**	**% 7.41 O_2 (1 sccm)**	**% 11.44 O_2 (1.5 sccm)**	**% 13.79 O_2 (2 sccm)**
1) (w-O-W) stretching mode	_	804,965	805,594	804,126
2) (w-o-W) stretching mode	_	711,399	714,545	708,881
3)(W-O-W) bending mode	_	300,42	300	300,629
4)(W-O-W) Bending mode	_	268,741	268,741	265,385
Si p-tipi	**% 4.45 O_2 (0.5 sccm)**	**% 7.41 O_2 (1 sccm)**	**% 11.44 O_2 (1.5 sccm)**	**% 13.79 O_2 (2 sccm)**
1) (W-O-W) Stretching mode	_	805,385	805,594	805,385
2) (W-O-W) Stretching mode	_	714,755	714,126	712,238
3) (W-O-W) bending mode	_	299,79	300,839	301,259
4) (W-O-W) bending mode	_	267,902	268,112	267,692

Table 3. FWHM of WO_3 thin films in Raman Spectroscopy

Si n-tipi	**% 4.45 O_2 (0.5 sccm)**	**% 7.41 O_2 (1 sccm)**	**% 11.44 O_2 (1.5 sccm)**	**% 13.79 O_2 (2 sccm)**
(W-O-W) stretching mode	_	24,71823	23,5692	30,94485
(W-O-W) stretching mode	_	29,81282	24,4564	31,11964
(W-O-W) bending mode	_	4,80163	10,48127	7,70834
(W-O-W) Bending mode	_	9,73598	12,22645	17,08973
Si p-tipi	**% 4.45 O_2 (0.5 sccm)**	**% 7.41 O_2 (1 sccm)**	**% 11.44 O_2 (1.5 sccm)**	**% 13.79 O_2 (2 sccm)**
(W-O-W) stretching mode	_	24,70637	23,60933	26,19571
(W-O-W) stretching mode	_	17,0363	21,83434	19,42854
(W-O-W) Bending mode	_	5,78893	7,22312	9,74574
(W-O-W) Bending mode	_	14,24921	9,9938	13,97798

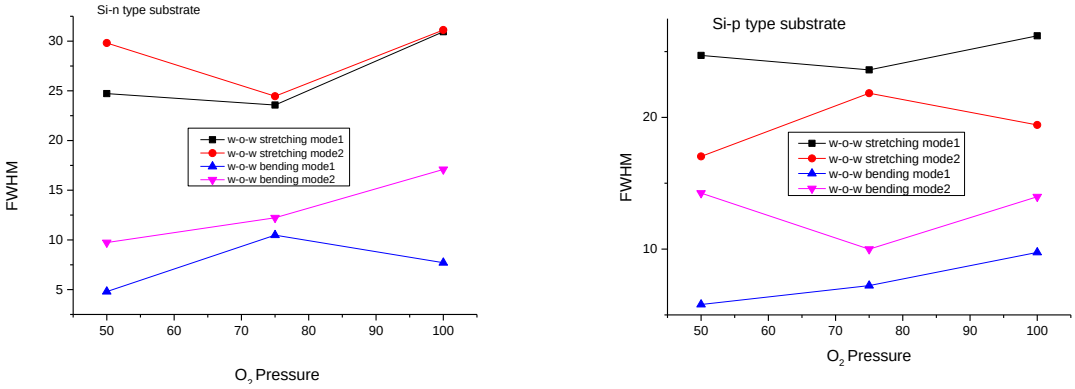


Figure 5. FWHM of WO3 thin films in Raman Spectroscopy for n and p type Si

4. Conclusion

To summarize, in the present study, the structural, optical properties and the electrochromic characteristics of oxygen sputtered WO_3 films have been investigated. WO_3 thin films were not shown 4.45% O_2 peaks whereas the best peaks were shown 11.44% O_2. Tungsten oxide is one of the most promising inorganic materials which exhibit excellent electrochromic, photochromic and gasochromic properties and it has been widely investigated to be used in electrochromic, gasochromic, solar energy, optical modulation, writing–reading–erasing optical devices.

References

[1] Regragui M, Jousseaume V, Addou M, Outzourhit A, Bernede J C and El-Idrissi B 2001 *Thin Solid Films* **397** 238–243
[2] Roth S, Ignatowitz M, Muller P, Monch W and Oesterschulze E, 2011 *Microelectronics J.* **88** 2349–2351
[3] Granqvist C G 2012 *Sol. Energy Mater. Sol. Cells* **99** 1–13.
[4] Mihelcˇicˇ M, Jerman I and Orel B 2013 *Prog. Org. Coat.* **76** 1752–1755.
[5] Dautremont-Smith W C 1982 *Displays* **3** pp 67-80.
[6] Goldner R B, Chapman R L, Foley G, Goldner E L, Haas T, Norton P, Seward G and Wong K K 1986 *Sol. Energy Mater*. **14** 195.
[7] Goldner R B, Brofos A, Foley G, Goldner E L, Haas T E, Henderson W, Norton P, Ratnam B A, Weis N and Wong K K 1984 *SPIE Proc*. **502** 54.
[8] Brezesinski T, Fattakhova-Rohlfing D, Sallard S, Antonietti M, and Smarsly B M 2006 *Small* **2(10)**, 1203
[9] Berveglieri G, Depero L, Groppelli S, and Nelli P 1995 *Sens. Actuators*, B 1 **26(1–3),** 89.
[10] Cantalini C, Sun H T, Faccio M, Pelino M, Santucci S, Lozzi L, and Passacantando M 1996 *Sens. Actuators*, B **31(1–2)**, 81
[11] Di Giulio M, Manno D, Micocci G, Serra A, and Tepore A 1997 *J. Phys. D: Appl. Phys*. **30(23),** 3211
[12] Tong M, Dai G, Wu Y, He X, Gao D and Mater J 2001 *Sci*. **36(10)**, 2535
[13] Agrawal A and Habibi H 1989, *Thin Solid Films* **169(2),** 257.
[12] LeGore L J Greenwood, O D Paulus, Frankel D J, Lad R J, Vac J 1997 *Sci. Technol*, A **15(3**), 1223.
[14] Tagtstrom P and Jansson U 1999 *Thin Solid Films* **352(1–2),** 107.
[15] Akram H, Tatsuoka H, Kitao M, and Yamada S 1987 *J. Appl. Phys*. **62(5)**, 2039.
[16] Kaneko H, Nishimoto S, Miyake S K, and Suedomi N 1986 *J. Appl. Phys.* **59(7)**, 2526.

[17] Kobayashi Y, Terada S, and Kubota K 1989 *Thin Solid Films* **168(1),** 133.
[18] Li M, Altman E I,Posadas A, and Ahn C H 2004 *Thin Solid Films* **446(2)**, 238.
[19] Garg A, Leake J A and Barbe Z H 2000 J.Phys. D: *Appl. Phys*. **33(9)**, 1048.
[20] Wang C, Sahu D R, Wang S, Chung-Kwei C and Huang J 2012 *J. Phys. D: Appl. Phys.* **45**, 225-303.
[21] Lu D Y, Chen J, Chen H J, Gong L, Deng S Z, Xu N S 2007 *Appl. Phys. Lett*, **90**, 041919
[22] Cazzanelli E, Vinegoni C, Mariotto G, Kuzmin A, Purans J 1999 *Sol. St. Ionics*, **123**, 67
[23] Zhou L, Ren Q J, Zhou X F, Tang J W, Chen Z H and Yu C Z 2008 *Microporous Mesoporous Mater* **109**, 248–257.
[24] Siciliano T, Tepore A, Micocci G, Serra A, Manno D and Filippo E 2008 Sens. *Actuators*, B **133**, 321–326.
[25] Hamberg L 1984 Indium tin oxide thin films: basic optical properties and applications to energy efficient windows, *Ph.D. Thesis*, *Chalmers University of Technology*, Gothenburg, Sweden.
[26] Born M, Wolf E 1983 *Principles of Optics* (Oxford: Pergamon Press)
[27] Heavens O S, 1970 *Optical Properties of Thin Films*, Dover, New York; Heavens O.S. 1965 *Thin Film Physics*, Methuen, London.
[28] Pankove J I, 1971 Optical Processes in Semiconductors, *Prentice- Hall, Englewood Cliffs*, N.J.
[29] Ozer N, Tepehan F, Tepehan G 1997 *Proc. SPIE—Int. Soc. Opt. Eng. (USA)* **3138**, 9–31.
[30] Miller E L, Paluselli D, Marsen B, Rocheleau R E 2004 *Thin solid Films* **466**, 307.